Quantifying Anthropomorphism of Robot Hands

Minas V. Liarokapis, Panagiotis K. Artemiadis and Kostas J. Kyriakopoulos

Abstract— **In this paper a comparative analysis between the human and three robotic hands is conducted. A series of metrics are introduced to quantify anthropomorphism and assess robot's ability to mimic the human hand. In order to quantify anthropomorphism we choose to compare human and robot hands in two different levels: comparing finger phalanges workspaces and comparing workspaces of the fingers base frames. The final score of anthropomorphism uses a set of weighting factors that can be adjusted according to the specifications of each study, providing always a normalized score between 0 (non-anthropomorphic) and 1 (human-identical). The proposed methodology can be used in order to grade the human-likeness of existing and new robotic hands, as well as to provide specifications for the design of the next generation of anthropomorphic hands. Those hands can be used for human robot interaction applications, humanoids or even prostheses.**

Index Terms: Anthropomorphism, Robot Hands, Kinematics, Workspace Analysis.

I. Introduction

Over the last years the field of robot hands design has received increased attention. Anthropomorphic characteristics (e.g. appearance, links lengths), use of light-weight, low-cost and flexible materials and synergistic actuation are some of the current trends. The aforementioned interest, is motivated by the fact that robot hands can be used to a number of everyday life applications, from myoelectric prostheses and teleoperation, to human robot interaction and humanoids. Despite the numerous studies conducted in the past in the field of robot hands design, there is a lack of information regarding anthropomorphism of robot hands. How can we define "anthropomorphism" ? Is it possible to discriminate if a robot hand is more anthropomorphic than another ? How can anthropomorphism be helpful ? Those are some of the fundamental questions that will be raised and addressed in this paper.

Minas V. Liarokapis and Kostas J. Kyriakopoulos are with the Control Systems Lab, School of Mechanical Engineering, National Technical University of Athens, 9 Heroon Polytechniou Str, Athens, 15780, Greece. Email: mliaro | kkyria @mail.ntua.gr

Panagiotis K. Artemiadis is with the ASU Human-Oriented Robotics and Control (HORC) Lab, School for Engineering of Matter, Transport and Energy, Ira A. Fulton Schools of Engineering, Arizona State University, 501 E. Tyler Mall, ECG 301, Tempe, AZ 85287-6106, USA. Email: panagiotis.artemiadis@asu.edu

This work has been partially supported by the European Commission with the Integrated Project no. 248587, THE Hand Embodied, within the FP7-ICT-2009-4-2-1 program Cognitive Systems and Robotics.

Regarding previous attempts to analyze the anthropomorphism of robotic hands, there are some interesting studies conducted in [1] and [2] where an index of anthropomorphism is proposed as the weighted sum of kinematics, contact surfaces and size scores. Although this study takes many robot attributes into consideration, it doesn't provide a workspace analysis of the human and the robot fingers, comparing them only in terms of number of fingers and phalanges available, and even more it doesn't incorporate fingers base frames mobility in the computation of the score of anthropomorphism. In [3] a review of performance characteristics for commercial prosthetic and anthropomorphic robotic hands is conducted. Authors perform a qualitative analysis, focusing on the mechanical characteristics of a wide set of robot hands.

Recent quantitative studies [4] and [5], use Gaussian Process - Latent Variable Models (GP-LVM) to represent in low-dimensional manifolds the human and robot hand workspaces and compare them. Authors use only fingertip positions in their analysis, without taking into account the configurations of the fingers, the lengths of the phalanges, or the mobility of the human fingers base frames, which is of outmost importance for specific grasp types. Regarding workspaces analysis, in [6] a comparison is performed between a haptic interface and the reachable workspace of the human arm, using the reachability map proposed in [7]. Such an analysis focuses on the position of the tool center point (TCP) in 3D space, discriminating not only the reachable and the dexterous workspaces as defined in [8] but also a capability map for the whole space, without taking into account the human to robot link-to-link comparison, that we want to perform for the case of the robot hand. Regarding human hand workspace analysis, in [9] the authors propose a methodology that can be used to quantify the functional workspace of the precision thumb - finger grasp, defined as the range of all possible positions in which thumb fingertip and each fingertip can simultaneously contact each other.

In this paper we propose a methodology for quantifying anthropomorphism of robot hands motion. We use a series of metrics based on finger workspace analysis assessing the relative coverages of human and robot finger phalanges workspaces as well as human and robot fingers base frames workspaces. The linear combination of the proposed metrics, can be adjusted according to the specification of the study resulting to a normalized score of anthropomorphism (i.e. human-likeness). Three different robotic hands are examined, in order to test the efficacy of the proposed methodology and a series of simulated paradigms of the different types of workspaces are provided.

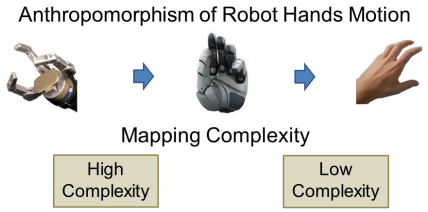

Fig. 1. Relationship between the mapping and anthropomorphism quantification problems.

The rest of the document is organized as follows: Section II focuses on the role and the different notions of anthropomorphism, Section III presents the human hand kinematic model, the robot hands and the correspondences between the human and robot fingers, Section IV focuses on the methods proposed to quantify anthropomorphism and compare robot hands in terms of human-likeness, Section V presents the results of the introduced metrics of anthropomorphism for a series of robot hands, while Section VI concludes the paper.

II. The Role of Anthropomorphism

The essence of anthropomorphism as described in [10], is "to imbue the imagined or real behavior of nonhuman agents with human-like characteristics, motivations, intentions and emotions". Anthropomorphism is derived from the Greek word *anthropos* (i.e. human) and the Greek word *morphe* (i.e. form). Regarding the perceived similarity, we can distinguish at least between two dimensions of similarity for anthropomorphism, similarity in motion and similarity in morphology. Recently we proposed *Functional Anthropomorphism* for human to robot motion mapping [11]. Functional anthropomorphism concerns a mapping approach that has as first priority to guarantee the execution of a specific functionality in task-space and then having accomplished such a prerequisite to optimize anthropomorphism of structure or form, minimizing some "distance" between the human and robot motion. The problem of quantifying anthropomorphism of robot hands motion is a "complementary" problem of mapping, because when a robotic artifact is "human-identical" the mapping problem becomes easy, as seen in Fig. 1.

But a justified question is: *Why do we need anthropomorphism in the first place ?* The last decade we experience an increasing demand for human robot interaction applications, so anthropomorphism becomes a necessity for two main reasons; safety and social connection through robot likeability. Moreover, for the case of robot hands, we must take into consideration the fact, that everyday life objects are designed to be manipulated by the human hand. Thus, the pursue of human-like design becomes a necessity not only to mimic the human hand in terms of appearance (morphological similarity), but also in order to incorporate in the robotic hand design those human specifications (e.g. kinematics), according to which the objects surrounding us have been crafted. Meeting those requirements, we will also manage to maximize robot hands ability to grasp and manipulate everyday life objects, following the "directions" provided by the nature's most versatile end-effector, the human hand.

III. Kinematics

A. Kinematic Model of the Human Hand

The kinematic model of the human hand that we use consists of 25 DoFs, five DoFs for the thumb, four DoFs for index and middle fingers and six DoFs for each one of the ring and pinky fingers. We use 6 DoFs for the ring and pinky fingers of the human hand model, in order to take into account the mobility of the carpometacarpal bones of the palm, that results to varying positions for the fingers base frames. Although human hand digit lengths, are quite easy to be measured, expressing the base of each finger relatively to the base of the wrist is a difficult problem, which requires advance techniques such as fMRI [12]. In this paper we use the parametric models for each human digit (derived from hand anthropometry studies) [13], [14] and [15], in order to define the lengths for all phalanges of the human hand. Moreover we incorporate the kinematics of the carpometacarpal bones as defined in [16], in the proposed human hand model in order to be able to compute the workspace of the human fingers base frames. The parametric models depend on specific parameters of the human hand that are the hand length (HL) and the hand breadth (HB). In this study we set both the HL and the HB parameters, to the mean value of the men and women 50th percentiles, according to the hand anthropometry study conducted in [17].

B. Robot Hands

Three quite different robot hands are examined in this study (due to space constraints). The five fingered DLR/HIT II (DLR - German Aerospace Center) [18], the Shadow Robot Hand (Shadow) [19] and the Barrett Hand (Barrett Technology Inc.) [20], that appear in Fig. 2.

Fig. 2. The robot hands examined in this study.

C. Defining the Correspondences between Human and Robot Hands Components

In this study, we consider each human and robot finger as a typical finger with two or three joints and three or four DoFs respectively (one for abduction/adduction and two or three for flexion/extension). In case that a robot finger has more degrees of freedom we consider that these DoFs contribute to the positioning of its base frame and we include them in the analysis during human and robot fingers base frames workspaces comparison. Thus human thumb is used for finger phalanges workspaces analysis, as a finger with two joints and three DoFs (one for abduction/adduction and two for flexion/extension) and the rest human fingers are used as fingers with three joints and four DoFs (one for abduction/adduction and three for flexion/extension). If a robot hand has fingers with more than four DoFs (e.g. the

pinky finger of Shadow hand [19]), we consider the rest as DoFs of the palm that contribute to the positioning of its fingers base frames. In order to compare human and robot fingers phalanges workspaces we must first define the correspondences between human and robot components. For example it's quite typical for a robot hand to have less than five fingers or less than three phalanges per finger [20]. To handle such situations we propose to map human to robot fingers with an order of significance starting from thumb and index, to middle, ring and pinky. Such a choice is justified by the fact that thumb, index and middle are the most important fingers participating in the various grasp types according to grasp taxonomy studies [21], [22], while ring and pinky appear to be subsidiary. Regarding the robot to human phalanges correspondence we follow a similar approach, assigning first the distal, then the proximal and finally the middle phalanx. In case that we have to find the correspondences for a robot hand with more than five fingers, we use the combination of consequent fingers that gives the highest score of anthropomorphism and if we have to find correspondences for a robot finger with more than three phalanges, we keep some joints fixed to zero, formulating those virtual phalanges that give once again the highest score of anthropomorphism.

IV. Methods

A. Convex Hulls

The convex hull of a set of points S in three dimensions is the intersection of all convex sets containing S. For N points $s_1, s_2, ..., s_N$, the convex hull C is given by the expression:

$$C \equiv \left\{ \sum_{k=1}^{N} a_k s_k : a_k \geq 0 \text{ for all } k \text{ and } \sum_{k=1}^{N} a_k = 1 \right\} \quad (1)$$

The convex hull of a finite point set $S \in R^n$ forms a convex polytope in R^n. Each $s \in S$ such that $s \notin Conv(S \backslash \{s\})$ is called a vertex of $Conv(S)$. In fact, a convex polytope in R^n is the convex hull of its vertices. When $S \in R^3$ as in our case, the convex hull is in general the minimal convex polyhedron $S \subseteq R^3$ that contains all the points in the set and which is the set of solutions to a finite system of linear inequalities:

$$P = \left\{ \mathbf{s} \in R^3 : \mathbf{As} \leq \mathbf{b} \right\} \quad (2)$$

where m is the number of half-spaces defining the polytope, $\mathbf{A}$ is an mxn matrix, $\mathbf{s}$ is an $nx1$ column vector of variables, and $\mathbf{b}$ is an $mx1$ column vector of constants. To compute the exact volume of a polytope P, it must be decomposed into simplices, following the simplex volume formula:

$$Vol(\Delta(s_1, ..., s_n)) = \frac{|\det(s_2 - s_1, ..., s_n - s_1)|}{n!} \quad (3)$$

where $\Delta(s_1, ..., s_n)$ denotes the simplex in R^n with vertices $s_1, ..., s_n \in R^n$. Moreover, when the triangulation method is used to decompose the polytope into simplices, then the volume of P is simply the sum of simplices volumes:

$$Vol(P) = \sum_{i=1}^{N} Vol(\Delta(i)) \quad (4)$$

There are plenty of methods available to compute the convex hull of a set S of points. In this study we choose to use the well known quickhull algorithm for convex hulls, that has been proposed in [23].

B. Quantifying Anthropomorphism of Robot Hands

In order to quantify anthropomorphism of robot hands, we must first answer the question *What are those characteristics that make the human hand the most dexterous and versatile end-effector known ?* One main advantage of the human hand, is its ability to move the fingers base frames, using the mobility of the carpometacarpal bones. More specifically, a series of power - prehensile grasps, such as the circular grasp or the lateral pinch, are typical examples, where the mobility of the human fingers base frames is of outmost importance. Thus, we choose to compare human and robot hands in two different levels: comparing finger phalanges workspaces and comparing human and robot fingers base frames workspaces.

1) Workspaces Computation: In order to quantify robot fingers anthropomorphism, we choose to perform a one-to-one comparison between the workspaces of human and robot fingers. For doing so, we need three sets of points S_D, S_M, $S_P \in R^3$ for each human and robot finger, that contain the boundary points of the workspaces of the distal, middle (i.e. intermediate) and proximal phalanges respectively. Human thumb doesn't have a middle phalanx, so the S_M point set is excluded, while thumb's workspace computation follows the same procedure. In order to conclude to these sets, we set some DoFs fixed to zero and we compute the forward kinematics of each finger while exploring the joint space of the moving DoFs. More specifically to compute set S_P we keep DoFs 3 and 4 fixed to zero, to compute set S_M we keep DoFs 2 and 4 fixed to zero and to compute S_D we keep DoFs 2 and 3 fixed to zero. DoF 1 (abduction/adduction) is always active, as it contributes to the workspaces of all phalanges. To proceed to workspace computation we discretize the joint space of active DoFs using a step of $\frac{R}{n}$, where usually n=20 degrees and R is the range of motion. Then we compute the forward kinematics for all n^2 possible configurations (where 2 is always the number of the active DoFs). S_P is the set containing all possible joint 2 positions as well as joint 1 static position, S_M is the set containing all possible joint 2 and joint 3 positions, while finally S_D is the set containing all possible joint 3 and fingertip positions. Then, the computed sets of points S_P, S_M and S_D are used to create the convex hulls of the phalanges workspaces, as depicted in Fig. 3.

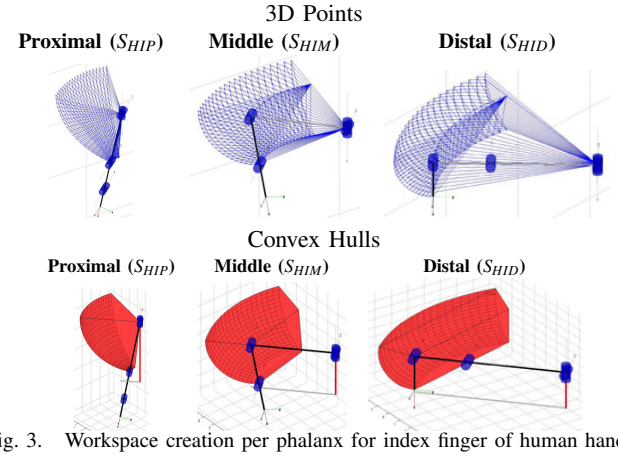

Fig. 3. Workspace creation per phalanx for index finger of human hand.

Regarding the computation of robot fingers base frames anthropomorphism, we choose to perform a one-to-one comparison between human and robot fingers base frames workspaces. Human and robot base frames differ not only in positions but also in orientations (relatively to the global reference frame at the center of the wrist), so in order to compute anthropomorphism of fingers base frames, we choose to compare human and robot finger bases frames positions and orientations workspaces. For doing so, we need a set of points S_{BFP} containing the boundary points of positions workspaces and a set S_{BFO} containing the boundary points of orientations workspaces (in S_{BFO} points are represented in euler angles). Once again, the workspaces are created using the palm forward kinematics and discretizing the joint space with a step of $\frac{R}{n}$ (usually n=20) degrees, where R is the range of motion. Such workspaces will be computed using the robot forward kinematics, only if the robot hand has at least one DoF contributing to the mobility of the fingers base frames. If robot base frames are fixed [18] then the fingers base frames positions "workspace" will be computed as the convex hull created by the five static robot fingers base frames positions, while the orientations "workspace" will be computed as the convex hull created by the five static robot fingers base frames orientations. Finally regarding forward kinematics, we use a simple and systematic approach to assign the DH parameters using any type of notation available (i.e. standard or modified), as described in [24].

2) Finger Phalanges Workspaces Comparison: Let S_{HID} be the set of points of the human index distal phalanx (HID) and S_{RID} the set of points of the robot index distal (RID) phalanx. We compute the convex hull of the human index distal phalanx workspace C_{HID}, and the convex hull of the robot index distal phalanx workspace C_{RID}. In order to quantify anthropomorphism of each robot finger, we propose to compare the workspaces of its phalanges with the workspaces of the equivalent human finger phalanges. Thus for index finger, we compute the intersection and the union of the human and robot workspaces for each phalanx. Let $C_{DI} = C_{RID} \cap C_{HID}$, be the intersection of the human and robot index distal phalanges workspaces and $C_{DU} = C_{RID} \cup C_{HID}$ be the union of the human and robot index distal phalanges workspaces. Then, anthropomorphism for the distal phalanx of index finger (A_{ID}) is computed as follows:[1]

$$A_{ID} = \frac{Vol(C_{DI})}{Vol(C_{DU})} 100\ (\%) \tag{5}$$

Equivalently for index finger, we quantify anthropomorphism for middle phalanx (A_{IM}) and proximal phalanx (A_{IP}).

3) Fingers Total Score: In order to conclude to the anthropomorphic score for the whole index finger (A_I), we use a weighted sum of the scores of its phalanges:

$$A_I = \frac{w_{ID}A_{ID} + w_{IM}A_{IM} + w_{IP}A_{IP}}{w_{ID} + w_{IM} + w_{IP}}\ (\%) \tag{6}$$

[1]In this paper we use a series of fractions with numerator always the volume of the intersection of the human and robot workspaces and denominator the volume of their union. So in order not to penalize the case a robot hand to be more dexterous than the human hand, if a robot hand has a joint with joint limits greater than human, we change them in order to be equal with the human limits.

where $w_{ID}+w_{IM}+w_{IP} = 1$, $w_{ID}, w_{IM}, w_{IP} \geq 0$ are the weights for each phalanx and can be set subjectively according to the specifications of each study. The same procedure can be used to quantify anthropomorphism of robot middle (A_M), robot ring (A_R), robot pinky (A_P) and robot thumb (A_T).

4) Fingers Base Frames Positions Comparison: In order to compute the level of anthropomorphism of the robot fingers base frames positions, we choose to compare the human and robot fingers base frames positions workspaces. For doing so, we use the convex hulls created by the human fingers base frames positions and the robot fingers base frames positions. Then, we compute the intersection of the human and robot fingers base frames positions convex hulls:

$$C_{BFPI} = C_{RBFP} \cap C_{HBFP} \tag{7}$$

where C_{RBFP} is the convex hull of the robot fingers base frames positions, C_{HBFP} is the convex hull of the human fingers base frames positions and C_{BFPI} is the convex hull of their intersection. The union of these convex hulls (C_{BFPU}), can be defined as:

$$C_{BFPU} = C_{HBFP} \cup C_{RBFP} \tag{8}$$

In order to compute the level of anthropomorphism of robot fingers base frames positions (A_{BFP}), we proceed as follows:

$$A_{BFP} = \frac{vol(C_{BFPI})}{vol(C_{BFPU})} 100\ (\%) \tag{9}$$

5) Fingers Base Frames Orientations Comparison: In order to compute the level of anthropomorphism of the robot fingers base frames orientations workspace, we choose to compare the convex hulls created by the human fingers base frames orientations and the robot fingers base frames orientations. More specifically we compute the intersection of the human and robot convex hulls:

$$C_{BFOI} = C_{RBFO} \cap C_{HBFO} \tag{10}$$

where C_{RBFO} is the robot fingers base frames orientations convex hull, C_{HBFO} is the human fingers base frames orientations convex hull and C_{BFOI} is the convex hull of their intersection. The union of human and the robot fingers base frames orientations convex hulls (C_{BFOU}), can be defined as:

$$C_{BFOU} = C_{HBFO} \cup C_{RBFO} \tag{11}$$

To compute the level of anthropomorphism of robot fingers base frames orientations (A_{BFO}), we proceed as follows:

$$A_{BFO} = \frac{vol(C_{BFOI})}{vol(C_{BFOU})} 100\ (\%) \tag{12}$$

6) Fingers Base Frames Total Score: In order to conclude to the fingers base frames total score, we use a weighted sum of the base frames positions score and the base frames orientations score, as follows:

$$A_{BF} = \frac{w_{BFP}A_{BFP} + w_{BFO}A_{BFO}}{w_{BFP} + w_{BFO}}\ (\%) \tag{13}$$

w_{BFP}, w_{BFO} are the base frames positions and orientations scores weights, where $w_{BFP}+w_{BFO} = 1$ and $w_{BFP}, w_{BFO} \geq 0$.

7) Total Score of Anthropomorphism: In order to compute the total score of anthropomorphism for each robot hand (A_R), we use a weighted sum of the computed scores for the robot fingers and the robot fingers base frames, as follows:

$$A_R = \frac{w_I A_I + w_M A_M + w_R A_R + w_P A_P + w_T A_T + w_{BF} A_{BF}}{w_I + w_M + w_R + w_P + w_T + w_{BF}}\ (\%) \tag{14}$$

where $w_I + w_M + w_R + w_P + w_T + w_{BF} = 1$, $w_I, w_M, w_R, w_P, w_T, w_{BF} \geq 0$ are the weights for the robot fingers scores and the robot fingers base frames score

respectively and can be also set subjectively according to the specifications of each study. Weights must be chosen according to the relative importance of each part of the hand. For example, the index, the middle and the thumb fingers can be considered more important that the ring and the pinky, while the fingers base frames weight must be quite high, because the ability of fingers base frames to move is a key factor of human hand's dexterity.

V. Results and Simulations

In order to compute and visualize the convex hulls as well as their unions and intersections we used the multiparametric toolbox (MPT) [25], together with the ninth version of Robotics Toolbox developed and distributed by Peter Corke [26]. In Fig. 4 the kinematic models of the human hand and the three robot hands are presented together with the convex hulls of their fingers base frames positions workspaces.

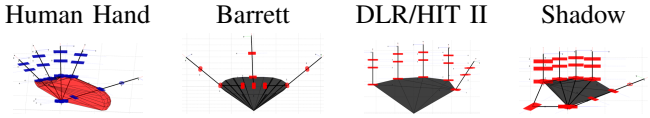

Fig. 4. Human hand and robot hands kinematic models and fingers base frames positions convex hulls.

Fig. 5 and Fig. 6 present comparisons between the fingers base frames positions workspaces and the fingers base frames orientations workspaces for human and robot hands, while Table I presents the score of anthropomorphism for each phalanx of each finger and the total score per finger.

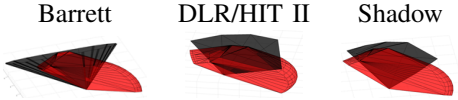

Fig. 5. Comparison of human hand (red) and robot hands (black) fingers base frames positions convex hulls. Results can be found in Table II.

Fig. 6. Comparison of human hand (red) and robot hands (black) fingers base frames orientations convex hulls. Results can be found in Table II.

Results in Table I are reported for all three robot hands and a hypothetical robot hand that "follows" human hand specifications, but with size equal to the 110% of the human hand (like DLR/HIT II). The fingers phalanges weights were set to $\frac{1}{3}$, except thumb phalanges weights that were set to $\frac{1}{2}$.

Table II presents the score of anthropomorphism of the palm's mobility quantified via the comparison of human and robot fingers base frames positions workspaces and fingers base frames orientations workspaces, for all five robot hands using weights: $w_{BFP} = \frac{1}{2}$ and $w_{BFO} = \frac{1}{2}$. Table III, presents the overall score of anthropomorphism for each robot hand, as the weighted sum of the aforementioned metrics, using weights: $w_I = 0.2, w_M = 0.2, w_R = 0.05, w_P = 0.05, w_T = 0.2, w_{BF} = 0.3$.

TABLE I

Score of Anthropomorphism for all Robot Hands and Hypothetical Robot Hand (HRobot), for Each Finger and Each Phalanx

Barrett

	Index	Middle	Ring	Pinky	Thumb
Proximal	18.89%	20.80%	-	-	0%
Middle	-	-	-	-	-
Distal	0%	0%	-	-	0%
Total	6.30%	6.93%	-	-	0%

DLR/HIT II

Proximal	46.50%	55.80%	67.74%	28.33%	16.35 %
Middle	40.86%	37.08%	65.60%	16.28%	-
Distal	34.33%	57.48%	76.02%	0.9%	0%
Total	40.56%	50.12%	69.79%	15.17%	8.18%

Shadow

Proximal	45.27%	43.02%	80.85%	49.18%	15.77%
Middle	40.86%	27.59%	53.43%	47.61%	-
Distal	52.81%	39.19%	70.21%	22.07%	22.72%
Total	46.31%	36.60%	68.16%	39.62%	19.25%

HRobot

Proximal	75.13%	75.13%	75.13%	75.13%	75.13%
Middle	86.49%	87.09%	86.93%	86.87%	-
Distal	66.55%	61.01%	57.42%	68.59%	88.66%
Total	76.06%	74.41%	73.16%	76.86%	81.90%

Shadow hand is reported to be the most anthropomorphic of the robot hands compared, mainly because of the mobility of the thumb and pinky fingers base frames. The high score of the hypothetical robot hand remains a goal for robot hand designers. Table IV assesses the effect of the workspace sampling resolution (expressed as the discretization of the range of motion R), on the score of anthropomorphism.

TABLE II

Score of Anthropomorphism of Fingers Base Frames for all Robot Hands and Hypothetical Robot Hand (HRobot)

	Barrett	DLR/HIT II	Shadow	HRobot
Positions	44.21%	16.85%	33.41%	75.13%
Orientations	7.34%	0.4%	60.67%	100%
Total	25.78%	8.62%	47.04%	87.57%

TABLE III

Total Score of Anthropomorphism for all Robot Hands and Hypothetical Robot Hand (HRobot)

Barrett	DLR/HIT II	Shadow	HRobot
10.38%	26.61%	39.93%	80.24%

TABLE IV

Effect of Workspace Sampling Resolution on Anthropomorphic Index Comparing Human vs Shadow Hand for all Index Finger Phalanges (R = Range of Motion)

Resolution	R/5	R/10	R/15	R/20	R/25	R/30
Score	46.564	46.331	46.300	46.288	46.284	46.282

Finally in Fig. 7, we present a comparison between the finger phalanges workspaces for the human hand and the three robot hands.

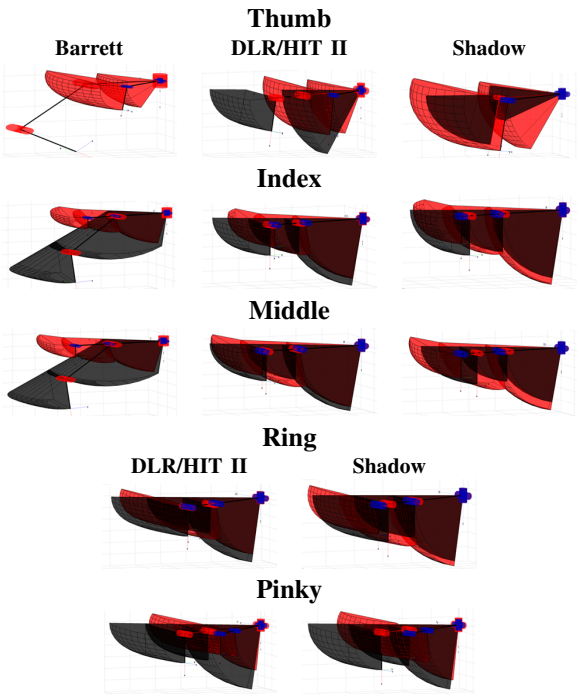

Fig. 7. Phalanges workspaces comparison for human hand (red convex hulls and blue kinematics chains) and robot hands (black convex hulls and red kinematic chains). The comparisons scores can be found in Table I.

VI. Discussion and Conclusions

In this paper we proposed a systematic approach to quantify anthropomorphism of robot hands. A comparison is performed taking into account those specifications that make the human hand the most dexterous and versatile end-effector known (e.g. opposable thumb, palm mobility etc.). More specifically we chose to compare human and robot hands in two different levels; comparing finger phalanges workspaces and comparing workspaces of the fingers base frames. The analysis was based on computational geometry and set theory methods. The efficacy of our method is validated, comparing three different robot hands against the human. The proposed methodology can be used not only to grade the human-likeness of specific robot hands, but also to provide specifications, for the design of a new generation of highly dexterous anthropomorphic robot hands. An open source toolbox implementing the proposed methods is available [27]. Regarding future directions we plan to extend the our study comparing more robot hands (e.g. like the ACT hand), as well as to take into account human synergies and possible synergistic characteristics[2], of the robot systems.

References

[1] L. Biagiotti, F. Lotti, C. Melchiorri, and G. Vassura, "How Far is the Human Hand? A Review on Anthropomorphic End Effectors," DIES Internal Report, University of Bologna, Tech. Rep., 2004.

[2] L. Biagiotti, "Advanced robotic hands: Design and control aspects," Ph.D. dissertation, Universita Degli Studi di Bologna, 2002.

[2]Human synergies - affecting the motion of the fingers and the mobility of the carpometacarpal bones - are not included in this study for simplicity reasons, but can be easily incorporated together with robot hands mechanical couplings [18], following the proposed procedure.

[3] J. Belter and A. Dollar, "Performance characteristics of anthropomorphic prosthetic hands," in *Rehabilitation Robotics (ICORR), 2011 IEEE International Conference on*, 29 2011-july 1 2011, pp. 1–7.

[4] T. Feix, "Anthropomorphic hand optimization based on a latent space analysis." PhD Thesis, Vienna University of Technology, 2011.

[5] T. Feix, J. Romero, C. Ek, H.-B. Schmiedmayer, and D. Kragic, "Grade your Hand Toolbox." [Online]. Available: http://grasp.xief.net/data/gradeHand.pdf

[6] F. Zacharias, I. S. Howard, T. Hulin, and G. Hirzinger, "Workspace comparisons of setup configurations for human-robot interaction." in *IROS*. IEEE, 2010, pp. 3117–3122.

[7] F. Zacharias, C. Borst, and G. Hirzinger, "Capturing robot workspace structure: representing robot capabilities," in *Intelligent Robots and Systems, 2007. IROS 2007. IEEE/RSJ International Conference on*, nov. 2 2007, pp. 3229–3236.

[8] J. J. Craig, *Introduction to Robotics: Mechanics and Control*, 3rd ed. Prentice Hall, 2004.

[9] L.-C. Kuo, H.-Y. Chiu, C.-W. Chang, H.-Y. Hsu, and Y.-N. Sun, "Functional workspace for precision manipulation between thumb and fingers in normal hands," *Journal of electromyography and kinesiology*, vol. 19, no. 5, pp. 829–839, oct 2009.

[10] N. Epley, A. Waytz, and J. Cacioppo, "On seeing human: A three-factor theory of anthropomorphism," *Psychological Review*, vol. 114, no. 4, pp. 864–886, October 2007.

[11] M. Liarokapis, P. Artemiadis, and K. Kyriakopoulos, "Functional anthropomorphism for human to robot motion mapping," in *IEEE International Symposium on Robot and Human Interactive Communication (RoMan)*, sept. 2012, pp. 31–36.

[12] G. Stillfried and P. van der Smagt, "Movement model of a human hand based on magnetic resonance imaging (MRI)," in *International Conference on Applied Bionics and Biomechanics, ICABB*, 2010.

[13] E. P. Pitarch, "Virtual human hand: Grasping strategy and simulation," Ph.D. dissertation, Universita Politechnica de Catalunya, 2007.

[14] B. Buchholz, T. J. Armstrong, and S. A. Goldstein, "Anthropometric data for describing the kinematics of the human hand," *Ergonomics*, vol. 35, no. 3, pp. 261–273, 1992.

[15] B. Buchholz and T. J. Armstrong, "A kinematic model of the human hand to evaluate its prehensile capabilities," *Journal of Biomechanics*, vol. 25, pp. 149–162, 1992.

[16] M. El-shennawy, K. Nakamura, R. M. Patterson, and S. F. Viegas, "Three-dimensional kinematic analysis of the second through fifth carpometacarpal joints," *The Journal of hand surgery*, vol. 26, no. 6, pp. 1030–1035, nov 2001.

[17] A. Poston, *Human engineering design data digest: human factors standardization systems / Human Factors Standardization SubTAG*. The Group, Washington, D.C, 2000.

[18] H. Liu, K. Wu, P. Meusel, N. Seitz, G. Hirzinger, M. Jin, Y. Liu, S. Fan, T. Lan, and Z. Chen, "Multisensory five-finger dexterous hand: The DLR/HIT Hand II," in *IEEE/RSJ International Conference on Intelligent Robots and Systems (IROS)*, Sept 2008, pp. 3692–3697.

[19] "Shadow Dexterous Hand C6M2 Technical Specification," Tech. Rep., 2012. [Online]. Available: http://www.shadowrobot.com/

[20] W. Townsend, "Barrett hand grasper," *Journal of Industrial Robots*, vol. 27, no. 3, pp. 181–188, 2000.

[21] T. Feix, R. Pawlik, H. Schmiedmayer, J. Romero, and D. Kragic, "A comprehensive grasp taxonomy," in *Robotics, Science and Systems: Workshop on Understanding the Human Hand for Advancing Robotic Manipulation*, June 2009. [Online]. Available: http://grasp.xief.net

[22] M. Cutkosky, "On grasp choice, grasp models, and the design of hands for manufacturing tasks," *Robotics and Automation, IEEE Transactions on*, vol. 5, no. 3, pp. 269–279, jun 1989.

[23] C. B. Barber, D. P. Dobkin, and H. Huhdanpaa, "The quickhull algorithm for convex hulls," *ACM Transactions on Mathematical Software*, vol. 22, no. 4, pp. 469–483, 1996.

[24] P. Corke, "A simple and systematic approach to assigning denavit - hartenberg parameters," *Robotics, IEEE Transactions on*, vol. 23, no. 3, pp. 590–594, june 2007.

[25] M. Kvasnica, P. Grieder, and M. Baotić, "Multi-Parametric Toolbox (MPT)," 2004. [Online]. Available: http://control.ee.ethz.ch/ mpt/

[26] P. Corke, "MATLAB toolboxes: robotics and vision for students and teachers," *Robotics Automation Magazine, IEEE*, vol. 14, no. 4, pp. 16–17, dec 2007.

[27] http://code.google.com/p/quantify-robots-anthropomorphism/, 2013, [Online; accessed 11-February-2013].